Detector Dependency of MODIS Polarization Sensitivity derived from on-orbit Characterization

Gerhard Meister[a], Bryan A. Franz[b], Ewa J. Kwiatkowska[c], Robert E. Eplee[d], and Charles R. McClain[b]

[a]Futuretech Corp., NASA Ocean Biology Processing Group, Code 614.2, Goddard Space Flight Center, Greenbelt, MD 20771, USA;
[b]NASA, Ocean Biology Processing Group, Code 614.2, Goddard Space Flight Center, Greenbelt, MD 20771, USA;
[c]TEC-EEP, European Space Agency (ESA), ESTEC, Keplerlaan 1, 2201 AZ Noordwijk ZH, The Netherlands;
[d]SAIC, NASA Ocean Biology Processing Group, Code 614.2, Goddard Space Flight Center, Greenbelt, MD 20771, USA;

ABSTRACT

Scanning radiometers on earth-orbiting satellites are used to measure the chlorophyll content of the oceans via analysis of the water-leaving radiances. These radiances are very sensitive to the atmospheric correction process, which in turn is polarization dependent. The image created by a scanning radiometer is usually composed of successive scans by two mirror sides and one or several detectors. The Moderate Resolution Imaging Spectroradiometer (MODIS) has 10 detectors for each ocean color band. If the polarization sensitivities are different among detectors and this is not taken account of in the atmospheric correction process, striping will occur in different parts of the images. MODIS polarization parameters were derived using ground truth data from another earth-orbiting sensor (Sea-viewing Wide Field-of-view Sensor, SeaWiFS), allowing a comparison of the on-orbit characterization and the prelaunch characterization. This paper presents these comparisons for the MODIS instruments on the Aqua and Terra satellites. The detector dependency is clearly different in the prelaunch characterization. This paper also describes the detector dependency of the vicarious corrections to the radiometric calibration coefficients. During the first four years of each mission, the only correction needed to minimize striping in the ocean color products is a constant offset, there is indication of a temporal trend or a view angle dependency for these offsets. The offsets are similar for both instruments, but larger in Terra.

Keywords: remote sensing, scanners, on-orbit calibration, vicarious calibration, polarization

1. INTRODUCTION

There are currently two units of the Moderate Resolution Imaging Spectroradiometer (MODIS)[1] orbiting the earth. The first was launched in December 1999 on NASA's Earth Observing System (EOS) Terra satellite, the second on the Aqua satellite in May 2002. MODIS has 36 spectral bands on four different focal planes. The Ocean Biology Processing Group (OBPG) at NASA uses bands 8-16 with center wavelengths from 412nm to 870nm to produce the standard ocean color data products.[2] The basic ocean color products are water-leaving radiances from bands 8-14 (412nm, 443nm, 488nm, 531nm, 551nm, 667nm, and 678nm). Bands 15 and 16 (748nm and 869nm) are used to determine the aerosol optical thickness and the aerosol type for atmospheric correction.

Each MODIS ocean color band has 10 independent detectors, and each of these detectors needs to be calibrated and characterized separately. Both MODIS instruments are calibrated using on-board calibrators[3] and lunar irradiances.[4] For MODIS Aqua, these calibration sources have been sufficient to produce high quality ocean color products.[2] For MODIS Terra, this has not been the case.[5] The OBPG has developed a vicarious calibration

Further author information:
G.M.: E-mail: Gerhard.Meister@nasa.gov

method to improve the MODIS Terra characterization for bands 8-14, using SeaWiFS[6] water-leaving radiances as truth fields.[7] The same method was applied to MODIS Aqua. This paper presents a comparison of the detector dependency of the results of these vicarious characterizations to independently measured prelaunch and on-orbit data. Such a comparison is useful for evaluating whether the traditional approaches to prelaunch characterization and on-orbit calibration are sufficient to produce ocean color products without image artifacts like striping.

2. STANDARD MODIS CALIBRATION AND CHARACTERIZATION METHODS

The standard MODIS calibration equation[3] uses the calibration coefficient m_1 to describe changes in the radiometric sensitivity of the instrument. The m_1's are used to derive earth scene reflectance factors ρ_{EV} from the measured counts of the earth scene (dn_{EV}) with:

$$\rho_{EV} \cdot \cos(\theta_{EV}) = m_1 \cdot dn^*_{EV} \cdot d^2_{Earth-Sun} \tag{1}$$

where ρ_{EV} are earth scene reflectance factors, dn^*_{EV} are the temperature corrected measured counts, and $d_{Earth-Sun}$ is the distance between earth and sun, and θ_{EV} is the solar zenith angle. The scan angle dependence is modeled by dividing by the RVS (response-versus-scan). In the vicarious cross calibration process, we chose to simplify the calibration approach by combining the effects of m_1 and RVS into one scan angle dependent variable, M11.

The calibration source for determining m_1 on-orbit is the solar diffuser. The solar diffuser is viewed at an angle of incidence on the scan mirror of 50.3°. The calibration source for determining the RVS are lunar measurements through the space view port. The moon is viewed at an angle of incidence on the scan mirror of 11.4°.[8] The radiometric response for all other angles of incidence is modeled, combining the solar diffuser, lunar, and prelaunch characterization measurements at various angles.

The standard polarization correction equation for an uncalibrated instrument[9] is

$$L_m = M_{11}L_t + M_{12}(Q_t cos2\alpha + U_t sin2\alpha) + M_{13}(-Q_t sin2\alpha + U_t cos2\alpha) + M_{14}V_t \tag{2}$$

where (L_t, Q_t, U_t, V_t) is the Stokes vector at the TOA, L_m is the measured radiance, and α is a rotation angle to adjust for different reference frames. Since V_t is very close to zero at the TOA, M_{14} is an irrelevant parameter for MODIS. The parameters M_{12} and M_{13} were determined prelaunch at scan angles from $-45°$ to $+45°$, for each band, mirror side, and detector.[10] The variations of these parameters with detector were considered suspect and not applied in the ocean color processing.[11]

In Kwiatkowska et al.,[7] M_{12} was the main polarization parameter retrieved in the vicarious calibration. However, the polarization correction equation for a calibrated instrument[9] is

$$L_m = L_t + m_{12}(Q_t cos2\alpha + U_t sin2\alpha) + m_{13}(-Q_t sin2\alpha + U_t cos2\alpha) + m_{14}V_t \tag{3}$$

with

$$m_{12} = \frac{M_{12}}{M_{11}} \tag{4}$$

$$m_{13} = \frac{M_{13}}{M_{11}} \tag{5}$$

For an instrument calibrated correctly with unpolarized light, M_{11}=1, and there is no need to distinguish between m_{12} and M_{12}. This assumption was used in Meister et al.[11] for MODIS Aqua. However, M_{11} is generally not equal to one for MODIS Terra. In the calculation of the polarization correction p_c (see eq. 18 of Meister et al.[11]), the measured radiance L_m should be replaced by L_m/M_{11} for $M_{11} \neq 1$. In this report and in the files containing the vicarious calibration results provided to specific users, m_{12} and m_{13} are used (instead of M_{12} and M_{13}), which can be directly used for eq. 18 of Meister et al.[11]

3. VICARIOUS CALIBRATION METHOD

The cross calibration method has been described by Kwiatkowska et al.,[7] so here we provide only a brief summary. For a given day, the level 3 water-leaving radiances from SeaWiFS are used to predict the top-of-atmosphere (TOA) radiances as seen by MODIS on that day, using the atmospheric correction approach from Gordon and Wang[12] in reverse mode.[13] All components of the Stokes vector (L, Q, U, V) are modeled. This allows not only a correction for the radiometric calibration parameters M_{11}, but also for the polarization correction parameters m_{12} and m_{13}. The modeled TOA radiances are compared to the radiances measured by MODIS for every scan angle, mirror side, and detector. This means that the instrument characterization parameters (M_{11}, m_{12}, m_{13}) can be derived as a function of scan angle, mirror side, and detector. To reduce noise, the scan angle dependence is modeled by a cubic function for M_{11}, as a linear function for m_{12} and m_{13}.

The retrieval of the instrument characterization parameters is repeated for one day in every month of the mission. This results in a time series for the instrument characterization parameters. Examples are shown below in Fig. 1 for m_{12} of bands 8 and 12, respectively. The results are smoothed over time using 5th order polynomials (see Fig. 4 in Kwiatkowska et al.[7]) before they are applied in the processing of ocean color products. The analysis in this paper starts with the unsmoothed values.

The retrievals for the parameter m_{13} showed a seasonal oscillation that could not be explained. No trend was seen in the m_{13} over the Terra or Aqua mission time frame, so the best choice was to use the m_{13} from the prelaunch characterization.[7]

Another choice we made was to calculate the M_{11} relative to the existing calibration, whereas the m_{12} and m_{13} were calculated absolute. E.g., for a value of M_{11}=0.99, the calibration coefficient m_1 in the standard radiometric calibration look-up table (e.g. LUT V5.0.35.1a for the Aqua vicarious calibration results) must be divided by 0.99. A vicarious value of e.g. $m_{12} = 0.02$ replaces the value in the standard polarization LUT. There are several other instrument parameters that in theory could be different from the prelaunch characterization, e.g. the relative spectral response, straylight sensitivity, linearity, temperature sensitivity, etc. We have no indication that any of these parameters should be adjusted for MODIS Terra, but we have not investigated this issue thoroughly. E.g., it is possible that the detector trend we found for the radiometric calibration coefficients (see Fig. 7 below) is partly due to a variation of the relative spectral response with detector.

4. DETECTOR DEPENDENCY OF THE POLARIZATION CORRECTION COEFFICIENTS

So far, there is no uncertainty analysis for the results of the vicarious calibration. The m_{12} as a function of time (before fitting the fifth order polynomial in time) are noisy (see Fig. 1), because m_{12} (and M_{11}) are derived independently for each month of the mission. There is no obvious trend in the first 4 years for either Terra or Aqua, so calculating the average and the standard deviation are reasonable approaches. In this paper, we will use the standard deviation as an uncertainty estimate, acknowledging that this estimate may either over or underestimate the true uncertainty. The resulting averages and standard deviations are shown in Figs. 2 to 4 as red diamonds and red error bars, resp. The black line shows the prelaunch m_{12}. The error bars on the prelaunch m_{12} are ± 0.005. This should be an overestimate, because the uncertainty of the polarization amplitude p_a as required by the MODIS specification is 0.5%, and since the polarization amplitude can be expressed as

$$p_a = \sqrt{m_{12}^2 + m_{13}^2} \tag{6}$$

an uncertainty for m_{12} of ± 0.005 basically assumes that m_{13} was determined with zero uncertainty.

Figs. 2 to 4 show that there are cases where the prelaunch characterization and the on-orbit characterization agree very well (e.g. for Terra band 8, all view angles), but there are other cases where we see a large offset between the two (e.g. for Aqua band 9, -45° view angle). At this point, it is not yet clear which characterization for MODIS Aqua is more accurate. For all bands and both sensors, agreement is good at $+45^\circ$ view angle for the edge detectors (detectors 1 and 10). The results for bands 11 and 14 are not shown, they are very similar to the results of bands 10 and 13, resp.

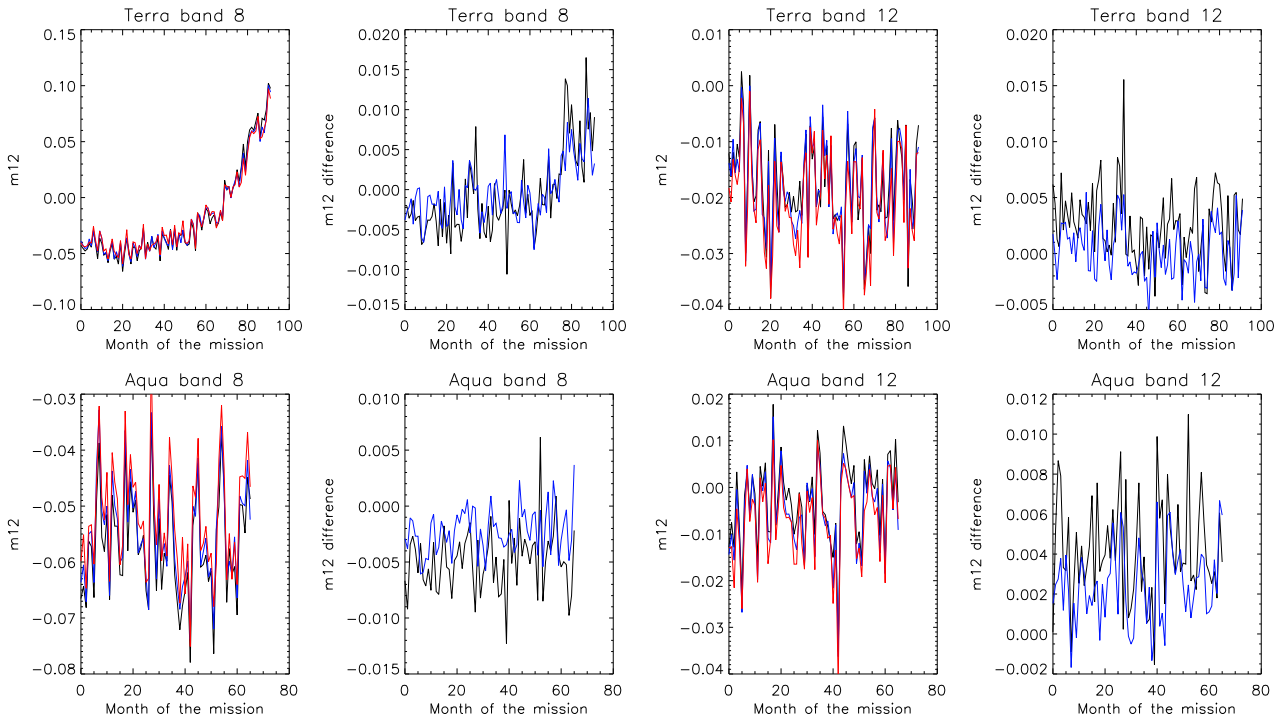

Figure 1. Vicariously determined m_{12} as a function of time for detectors 1, 5, and 10 (black, blue, red, resp.) and difference of m_{12} of detector 1 minus detector 10 (black) and detector 1 minus detector 5 (blue). Data for bands 8 and 12, mirror side 1, nadir viewing. MODIS Terra data on top, MODIS Aqua on bottom.

Another obvious difference between the prelaunch characterization and the on-orbit characterization is that the detector dependence is very small in all bands for the on-orbit characterization, whereas for the prelaunch characterization, the m_{12} of the central detectors (3-8) are higher than those of the edge detectors (1 and 10) for bands 10-13, by up to 1%. For band 8, both characterizations show a small increase (about 0.5%) of m_{12} with increasing detector number.

The relative uncertainty of the detector dependence of the on-orbit characterization is expected to be smaller than indicated by the error bars in Figs. 2 to 4, which are more indicative of the absolute error. As is shown in Fig. 1, most of the noise in the m_{12} time series is correlated between detectors. Table 1 presents the calculated mean and standard deviations of the m_{12} differences of certain detector pairs. E.g. the average in the first column is calculated as

$$< (m_{12}^{\mathrm{Det.1}} - m_{12}^{\mathrm{Det.5}}) >= \frac{1}{n_M} \cdot \sum_{i=1}^{n_M} (m_{12,i}^{\mathrm{Det.1}} - m_{12,i}^{\mathrm{Det.5}}) \tag{7}$$

where $m_{12,i}^{\mathrm{Det.1}}$ is the m_{12} of the i-th month of the mission for detector 1, and $n_M = 48$ is the number of months of the time series.

Table 1 shows that the average detector difference between detectors 1 and 5 is very small, and the standard deviation is on the same order of magnitude. E.g. for band 12, the difference is 0.001 for Terra and 0.002 for Aqua, with a standard deviation of 0.002 in both cases. This suggests that the detector dependence of m_{12} is on the order of 0.2%. On the other hand, the prelaunch characterization shows a difference of about 1% between detectors 1 and 5, see Fig. 3.

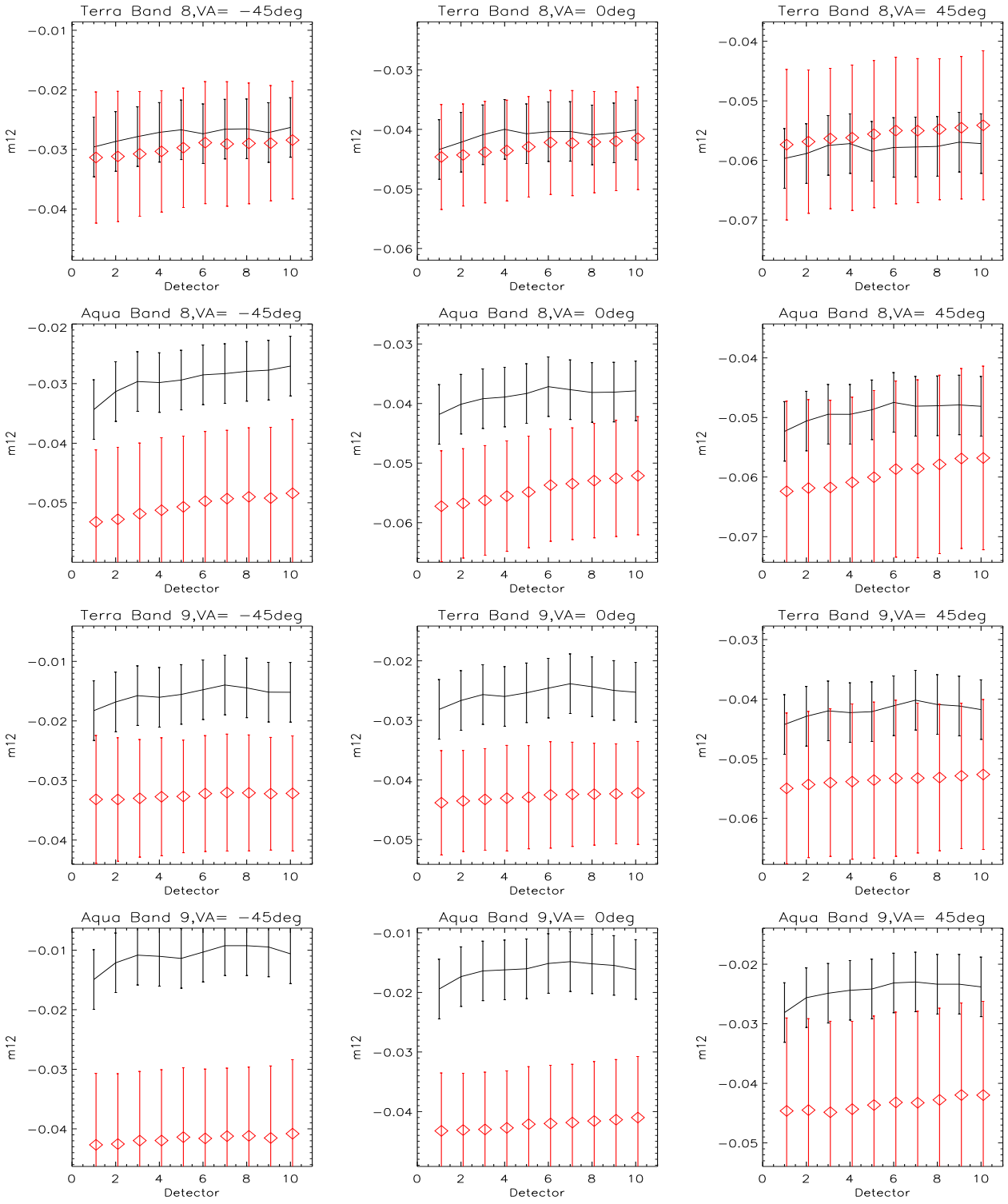

Figure 2. Comparison of prelaunch m_{12} (solid black line) and vicarious m_{12} (red diamonds) for view angles of $-45°$, nadir, and $+45°$ for MODIS Terra and MODIS Aqua, bands 8 and 9.

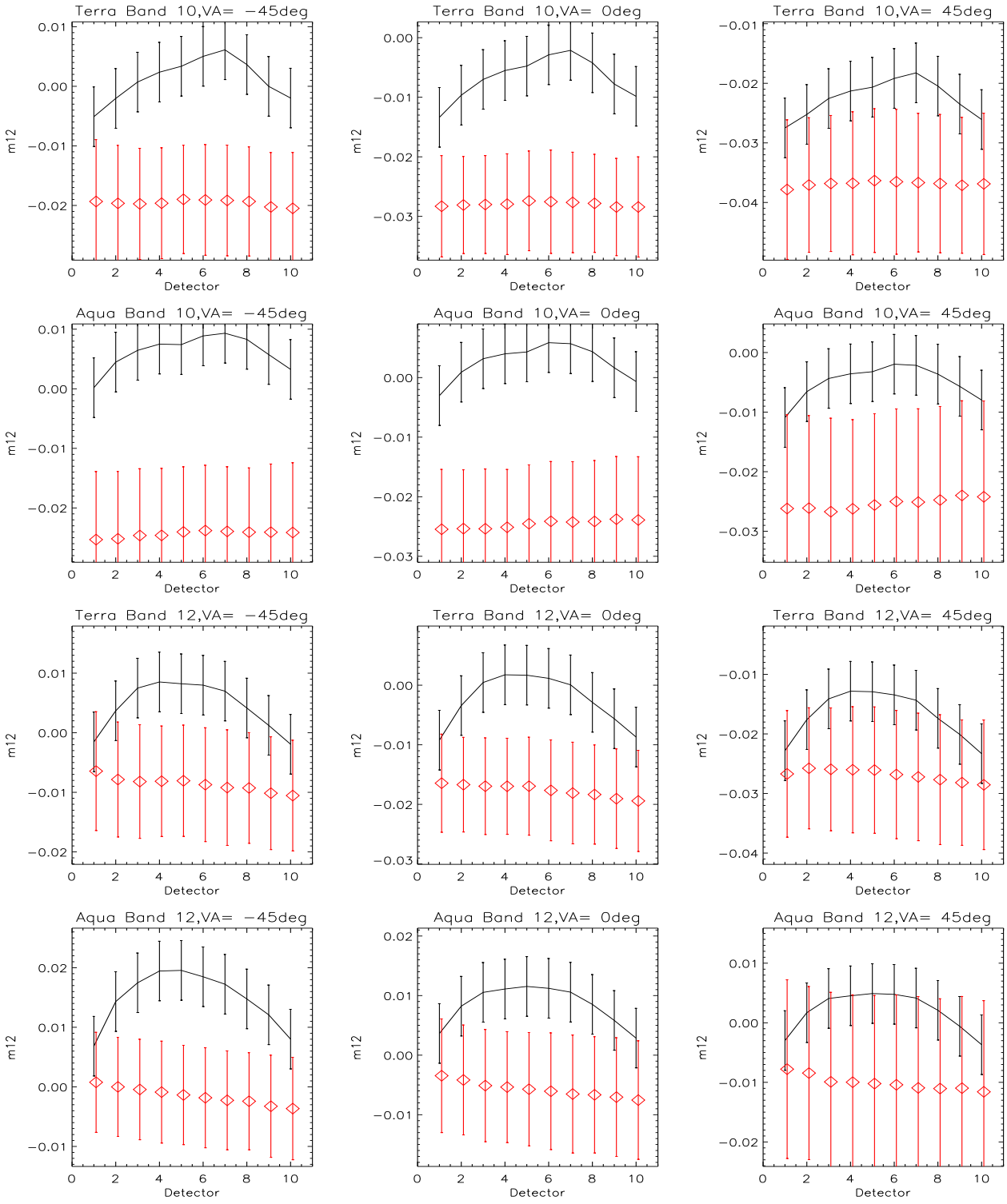

Figure 3. Comparison of prelaunch m_{12} (solid black line) and vicarious m_{12} (red diamonds) for view angles of $-45°$, nadir, and $+45°$ for MODIS Terra and MODIS Aqua, bands 10 and 12.

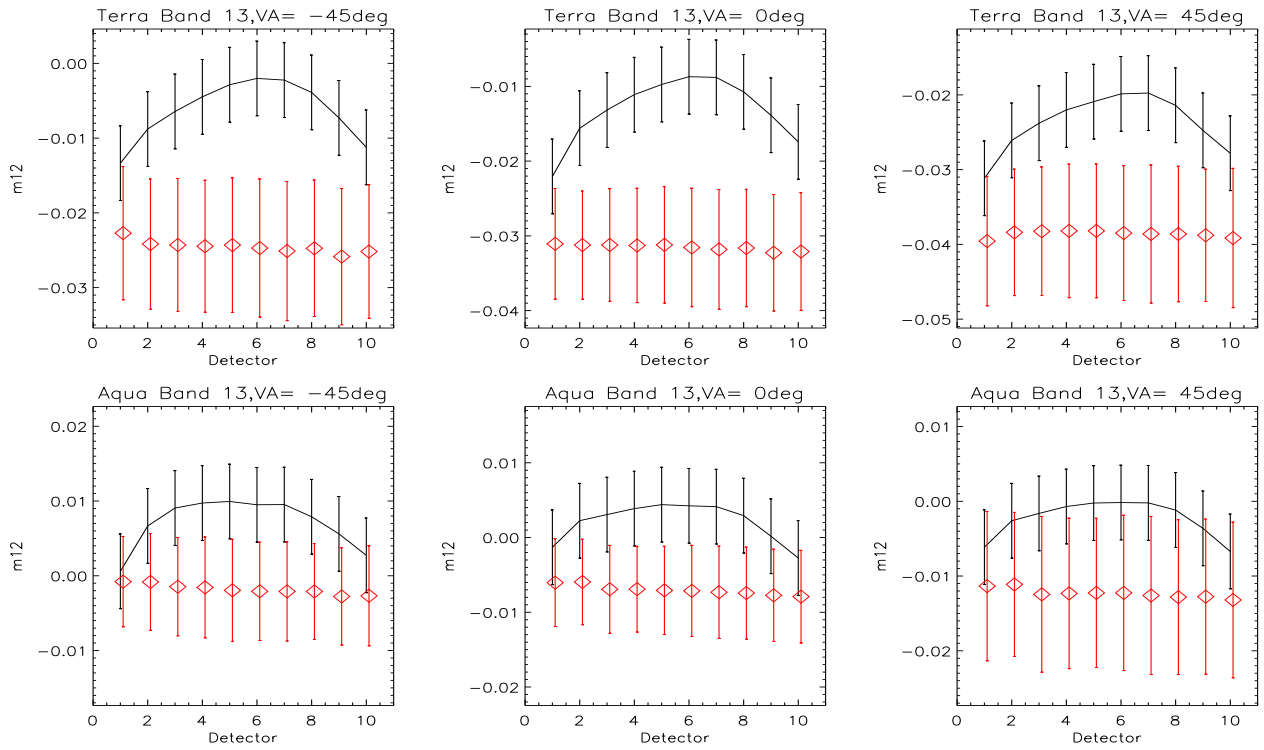

Figure 4. Comparison of prelaunch m_{12} (solid black line) and vicarious m_{12} (red diamonds) for view angles of -45°, nadir, and $+45^\circ$ for MODIS Terra and MODIS Aqua, band 13.

5. DETECTOR DEPENDENCY OF THE RADIOMETRIC CALIBRATION COEFFICIENTS

5.1 Verification with lunar measurements

The Terra cross calibration results are relative to a calibration that used band-averaged lunar measurements.[14] Fig. 5 compares the detector trends from the vicarious calibration at the lunar view angle to the trends from detector specific lunar trending. It can be seen that the overall trends agree very well:

- both mirror sides show the same detector trends for detectors 1 and 10 until the middle of the mission
- starting from the middle of the mission, M_{11} of detector 10 decreases by about 2.5% more than detector 1 for mirror side 1

Table 1. Mean and standard deviation for detector differences from m_{12} of detector 1 for the first 4 years of on-orbit data (i.e. 48 data points used for the calculation of each mean and standard deviation) for nadir (frame 677).

Band	Mean Det. 1-5 Terra	Stdev. Det. 1-5 Terra	Mean Det. 1-10 Terra	Stdev. Det. 1-10 Terra	Mean Det. 1-5 Aqua	Stdev. Det. 1-5 Aqua	Mean Det. 1-10 Aqua	Stdev. Det. 1-10 Aqua
8	-0.002	0.002	-0.003	0.003	-0.002	0.002	-0.005	0.003
9	-0.001	0.003	-0.002	0.003	-0.001	0.002	-0.002	0.002
10	-0.001	0.002	0.000	0.003	-0.001	0.002	-0.002	0.003
11	0.001	0.002	0.004	0.003	0.003	0.002	0.004	0.003
12	0.001	0.002	0.003	0.003	0.002	0.002	0.004	0.003
13	0.000	0.002	0.001	0.003	0.001	0.002	0.002	0.002

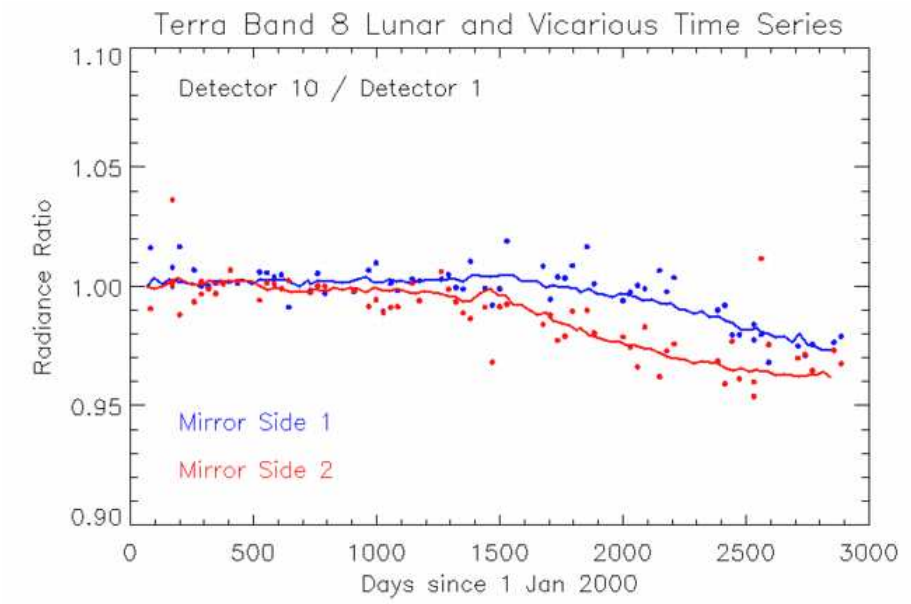

Figure 5. Ratio of detector 10 over detector 1 for Terra M_{11} as derived from vicarious calibration (solid line) and lunar measurements (dots) for each mirror side.

- starting from the middle of the mission, M_{11} of detector 10 decreases by about 4% more than detector 1 for mirror side 2

These results are very encouraging, because they confirm the validity of the results of the vicarious calibration method through independent measurements.

5.2 View angle dependency

A similar analysis as for the polarization coefficient m_{12} in section 4 can be done for the unpolarized gain correction coefficient M_{11}. Fig. 6 shows the M_{11} as a function of time for MODIS Terra and Aqua. It can be seen that in the first 48 months of the mission, the detectors of Terra band 8 do not show a clear trend relative to each other, but they all decrease by about 5%. It is therefore somewhat problematic to deduce any detector dependency based on the assumption of absolute stability of the M_{11} in the first 48 months. On the other hand, for MODIS Aqua, there is no obvious temporal trend for band 8. There is a variation of about 0.5% for Aqua band 12 in the first 48 months. The variation is sufficiently small to not interfere substantially with the analysis. As will be shown below, even the large decrease of MODIS Terra band 8 allows reasonable results.

The MODIS Terra M_{11} averages over the first 48 months are shown in Fig. 7. The Terra vicarious calibration was calculated relative to a calibration table where no destriping correction had been applied. It can be seen that the corrections from the Terra vicarious calibration are qualitatively similar to the MODIS Aqua operational detector corrections that were derived with a different method,[15] but often the corrections are larger for Terra. The Terra corrections continuously decrease with detector (except for band 13, detector 10), whereas the MODIS Aqua corrections decrease from detector 1 to detector 5, and then usually remain relatively stable from detectors 6 to 10 (but increase for band 8). The view angle dependency of the Terra M_{11} relative detector trends is very small (i.e. the curves for the different view angles have a very similar shape), but the mean of the 10 detectors varies strongly with view angle.

The MODIS Aqua M_{11} averages over the first 48 months are shown in Fig. 8. The Aqua vicarious calibration was calculated relative to a calibration table where the destriping correction had been applied, i.e. the detector trend shown by the diamonds in Fig. 7 has already been removed. It can be seen that the remaining trends with detector are all contained within $\pm 0.1\%$ for each view angle. This demonstrates excellent consistency between

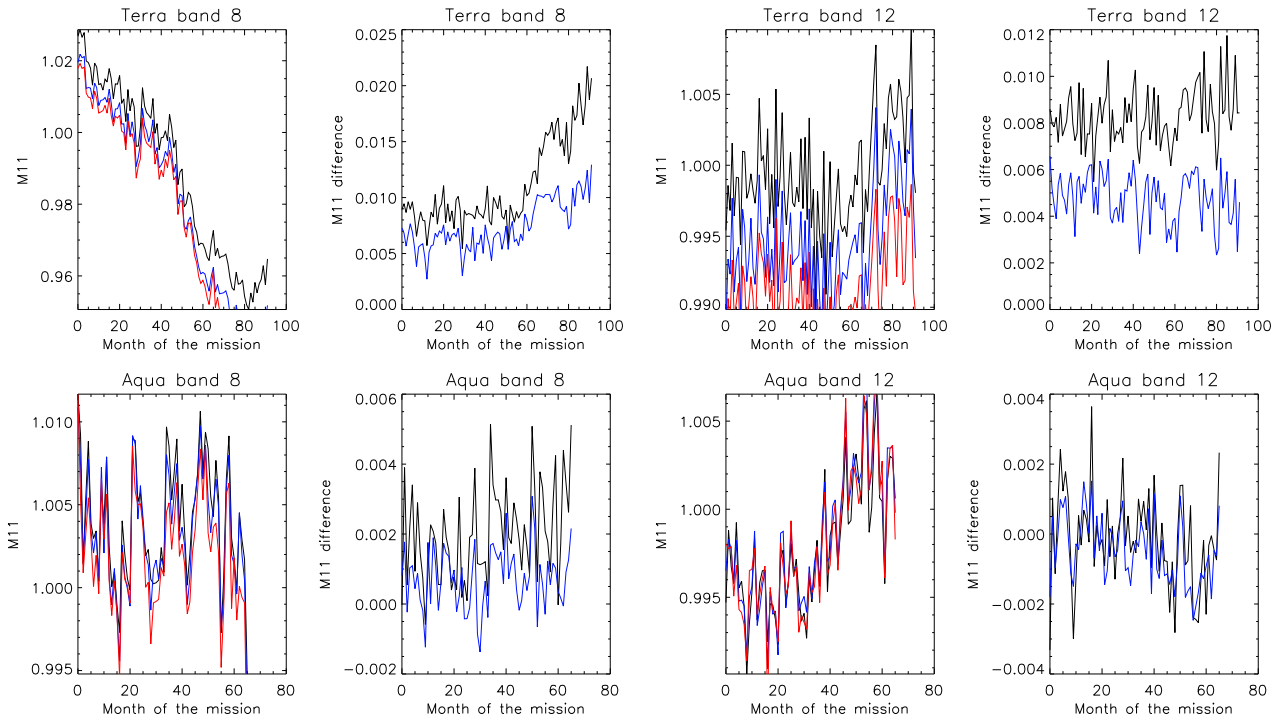

Figure 6. Vicariously determined M_{11} as a function of time for detectors 1, 5, and 10 (black, blue, red, resp.) and difference of M_{11} of detector 1 minus detector 10 (black) and detector 1 minus detector 5 (blue). Data for bands 8 and 12, mirror side 1, nadir viewing. MODIS Terra data on top, MODIS Aqua on bottom.

the two approaches. The two approaches are also consistent with the detector dependency derived from lunar measurements, see green triangles in Fig. 7. The lunar detector residuals were derived with a similar methodolgy as in Xiong et al.,[16] but for the first 48 months of each mission. The agreement between the Terra lunar detector residuals (black triangles in Fig. 7) and the Terra vicarious calibration results is also very good.

Generally, detector 4 in Fig. 8 is elevated, which is probably related to a known instability of the band 16 detector 4 gain, see Fig.3 in Meister et al., 2006,[15] which may influence the other bands via the atmospheric correction algorithm used in the vicarious calibration and in the analysis for the operational destriping.[15] Possibly there is a residual trend for band 8, view angles $-45°$ and $0°$, where detector 1 is about 0.2% higher than detector 10. Nevertheless, the very small residuals show that the application of a time and view angle independent detector correction as described in Meister et al., 2006[15] is justified for the first four years of MODIS Aqua.

6. DISCUSSION AND CONCLUSIONS

Evidence was presented in Meister et al.[11] that the detector dependence of the MODIS Aqua prelaunch polarization characterization measurements is suspect, based on the characterization measurements themselves (measurements from $-180°$ to $0°$ have a different mean value than measurements from $0°$ to $+180°$, no clear two-cycle pattern in many bands, four-cycle pattern sometimes stronger than two-cycle pattern, inconsistent detector dependence of the four-cycle pattern).

Aqua and Terra vicarious characterization results (using SeaWiFS data as a calibration source) show a very small detector dependence of the polarization coefficient m_{12} for all bands, contrary to the prelaunch characterization of bands 10-13. The large detector dependence of the prelaunch characterization for bands 10-13 is most likely caused by characterization artifacts and should not be applied to ocean color processing. Most likely, the detector dependence of bands 14-16 in the prelaunch measurements is erroneous as well. On the

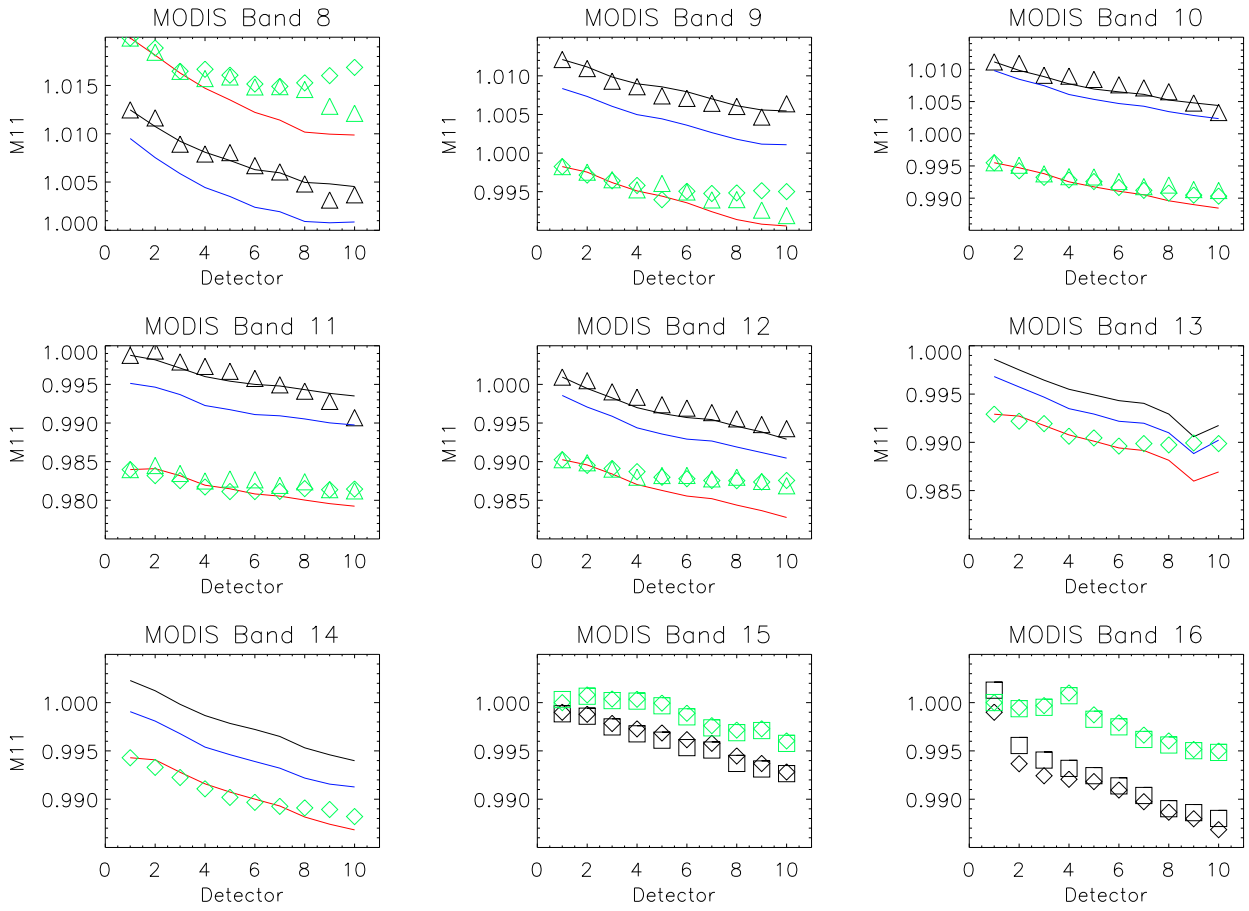

Figure 7. Time-averaged vicarious M_{11} for view angles of $-45°$, nadir, and $+45°$ (black, blue, red solid line, resp.) for MODIS Terra bands 8-14, mirror side 1. The black (green) triangles show the detector residuals of the Terra (Aqua) lunar analysis. The green diamonds show the MODIS Aqua detector corrections from the operational processing. The values of the black (green) symbols have been normalized so that detector 1 equals detector 1 of the black (red) line. MODIS bands 13-16 saturate when viewing the moon, so no triangles are shown for those bands. No M_{11} were derived for bands 15 and 16. For those two bands, the green diamonds (squares) show the MODIS Aqua detector corrections from the operational processing for mirror side 1 (2), the black diamonds (squares) show the MODIS Terra detector corrections for mirror side 1 (2) that were applied in the calibration LUT V5.0.38.1c (the MODIS Terra M_{11} were derived relative to this LUT) to bands 15 and 16 only. The MODIS Terra detector corrections were derived with the same method as described in Meister et al.[15] for MODIS Aqua. The detector corrections of both mirror sides are plotted relative to detector 1 of mirror side 1 for each sensor, the normalization of detector 1 of mirror side 1 itself is arbitrary.

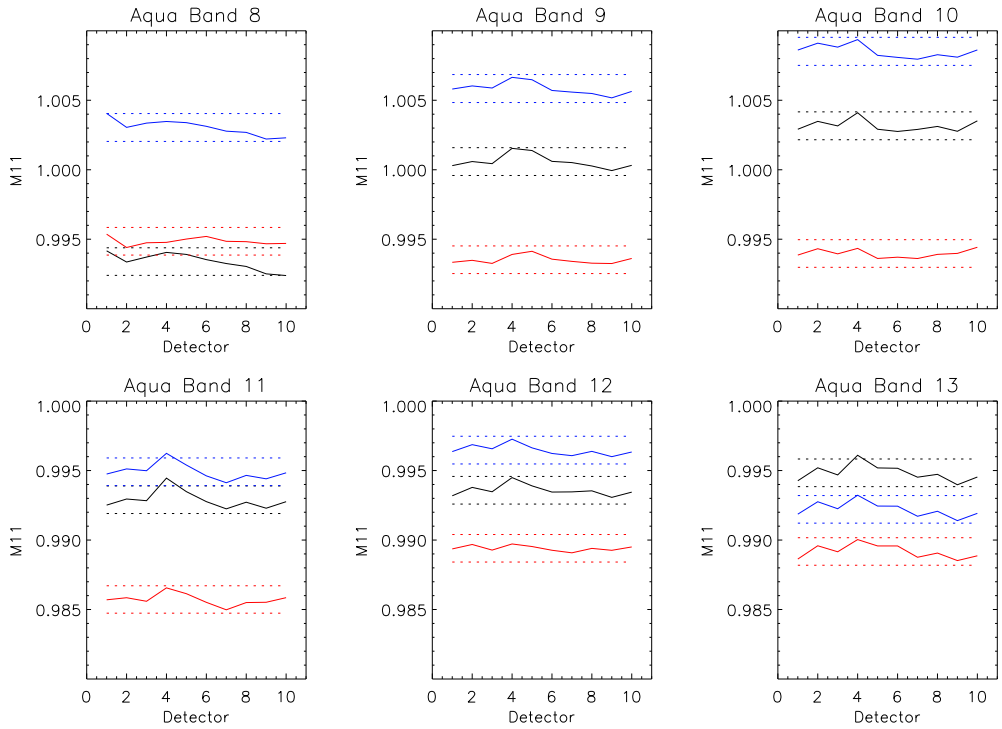

Figure 8. Time-averaged vicarious M_{11} for view angles of $-45°$, nadir, and $+45°$ (black, blue, red solid line, resp.) for MODIS Aqua bands 8-13, mirror side 1. The dashed lines show the mean over the ten detectors $\pm 0.1\%$.

other hand, the small detector dependence of bands 8 and 9 was also found in the on-orbit characterization, and an application of the detector trend for these two bands could result in reduced striping in ocean color imagery.

The relative detector temporal trends of the M_{11} (radiometric gain correction coefficients) from the MODIS vicarious calibration results are confirmed by independent lunar measurements for both Terra and Aqua, which confirms the validity of the vicarious calibration approach.

For MODIS Aqua, the vicarious calibration results for M_{11} justify the implementation of a destriping correction independent of view angle and time as proposed in Meister et al.[15] for the first four years of the Aqua mission (2002-2006). Constant offsets between the detectors are all that is needed. There is evidence (not shown here) that since 2008, this approach does not yield satisfying results anymore for band 8.

According to the vicarious calibration results, in the first four years of the mission, MODIS Terra had similar relative detector trends as MODIS Aqua:

- the detectors relative to each other were stable in the first 4 years after applying the detector dependent solar diffuser calibration,
- the view angle dependency was negligible.

So for both sensors, constant offsets between the detectors are sufficient to reduce striping in the ocean color products. However, MODIS Terra requires substantial corrections to the calibration coefficients that are common to all detectors.

ACKNOWLEDGMENTS

We want to thank our colleagues from MCST and OBPG for their support. This work was funded by the NASA MODIS Science Team.

REFERENCES

[1] Barnes, W. L., Pagano, T. S., and Salomonson, V. V., "Prelaunch characteristics of the moderate resolution imaging spectroradiometer (MODIS) on EOS-AM1," *IEEE Transactions on Geoscience and Remote Sensing* **36**(4), 1088–1100 (1998).

[2] Franz, B. A., Werdell, P. J., Meister, G., Bailey, S. W., Eplee, R. E., Feldman, G. C., Kwiatkowska, E., McClain, C. R., Patt, F. S., and Thomas, D., "The continuity of ocean color measurements from SeaWiFS to MODIS," *Proc. SPIE* **5882**(1), 58820W, SPIE (2005).

[3] Xiong, X. and Barnes, W. L., "An overview of MODIS radiometric calibration and characterization," *Advances in Atmospheric Sciences* **23**(1), 69–79 (2006).

[4] Sun, J., Xiong, X., Barnes, W., and Guenther, B., "MODIS reflective solar bands on-orbit lunar calibration," *IEEE Transactions on Geoscience and Remote Sensing* **45**(7), 2383–2393 (2007).

[5] Franz, B. A., Kwiatkowska, E. J., Meister, G., and McClain, C. R., "Moderate resolution imaging spectroradiometer on terra: limitations for ocean color applications," *Journal of Applied Remote Sensing* **2**, 023525 (2008).

[6] McClain, C. R., Feldman, G. C., and Hooker, S. B., "An overview of the SeaWiFS project and strategies for producing a climate research quality global ocean bio-optical time series," *Deep-Sea Research II* **51**, 5–42 (2004).

[7] Kwiatkowska, E. J., Franz, B. A., Meister, G., McClain, C. R., and Xiong, X., "Cross calibration of ocean-color bands from Moderate-Resolution Imaging Spectroradiometer on Terra platform," *Applied Optics* **47**(36), 6796–6810 (2008).

[8] Eplee, R. E., Xiong, X., Sun, J.-Q., Meister, G., and McClain, C. R., "The cross calibration of SeaWiFS and MODIS using on-orbit observations of the moon," in [*Earth Observing Systems XIV*], Butler, J. J. and Xiong, J., eds., *Proc. SPIE* **7452**, 745235 (2009).

[9] Gordon, H. R., Du, T., and Zhang, T., "Atmospheric correction of ocean color sensors: analysis of the effects of residual instrument polarization sensitivity," *Applied Optics* **36**(27), 6938–6948 (1997).

[10] Sun, J. and Xiong, X., "MODIS polarization sensitivity analysis," *IEEE Transactions on Geoscience and Remote Sensing* **45**(9), 2875–2885 (2007).

[11] Meister, G., Kwiatkowska, E. J., Franz, B. A., Patt, F. S., Feldman, G. C., and McClain, C. R., "Moderate-resolution imaging spectroradiometer ocean color polarization correction," *Applied Optics* **44**(26), 5524–5535 (2005).

[12] Gordon, H. R. and Wang, M., "Retrieval of water-leaving radiance and aerosol optical thickness over the oceans with SeaWiFS: A preliminary algorithm," *Appl. Opt.* **33**, 443–452 (1994).

[13] Franz, B. A., Bailey, S. W., Werdell, P. J., and McClain, C. R., "Sensor-independent Approach to the Vicarious Calibration of Satellite Ocean Color Radiometry," *Applied Optics* **46**, 5068–5082 (August 2007).

[14] Xiong, X., Sun, J., Meister, G., Kwiatkowska, E., and Barnes, W. L., "Characterization of MODIS VIS/NIR spectral band detector-to-detector differences," *Proc. SPIE* **7081**, 70810C (2008).

[15] Meister, G., Kwiatkowska, E. J., and McClain, C. R., "Analysis of image striping due to polarization correction artifacts in remotely sensed ocean scenes," *Proc. SPIE* **6296**(1), 629609 (2006).

[16] Xiong, X., Sun, J., Barnes, W., Guenther, B., and Salomonson, V., "Inter-comparison study of terra and aqua MODIS reflective solar bands using on-orbit lunar observations," *NEWRAD 2005, 9th International Conference on New Developments and Applications in Optical Radiometry, October 17 - 19* (2005).